JOC*Article*

Synthesis and Conformational Analysis of Small Peptides Containing 6-*Endo*-BT(t)L Scaffolds as Reverse Turn Mimetics

Andrea Trabocchi,[†] Ernesto G. Occhiato,[†] Donatella Potenza,[‡] and Antonio Guarna*[,†,§]

Dipartimento di Chimica Organica "Ugo Schiff", Università di Firenze, Polo Scientifico di Sesto Fiorentino, Via della Lastruccia 13, I-50019 Sesto Fiorentino, Firenze, Italy, Istituto di Chimica dei Composti Organo Metallici, Via Jacopo Nardi 39, I-50132 Firenze, Italy, and Dipartimento di Chimica Organica e Industriale, Università di Milano, Via Venezian 21, I-20133 Milano, Italy

antonio.guarna@unifi.it.

Received March 27, 2002

Two new dipeptide isosteres derived from L-leucine and *meso*-tartaric acid derivatives, named 6-*endo*-BTL and 6-*endo*-BtL, were inserted in a small peptide by means of SPPS, and the conformational features of the resulting peptides **3** and **4** were studied by NMR, IR, and molecular modeling techniques. The presence of a reverse turn conformation was observed in all the structures, suggesting the key role of the scaffolds as reverse turn promoters. Peptides **3** and **4** did not adopt a preferred conformation as indicated by the presence of equilibria between open turn and intramolecular hydrogen-bonded structures. 6-*endo*-BTL-peptide **3** showed a 3:1 mixture of conformers. The major conformer adopted mainly an open turn structure in equilibrium with hydrogen-bonded structures. The minor conformer displayed a better organized structure with a 14-membered ring hydrogen-bond typical of a β-hairpin-like structure, in equilibrium with a γ-turn, too. 6-*endo*-BtL-peptide **4** showed a unique conformer, and did not adopt as good a conformation as **3**, due to the bulky equatorial substituent at C-2. Thus, marked structural differences between peptides containing 6-*endo*-BTL and 6-*endo*-BtL scaffolds as reverse turn inducers exist.

Introduction

Reverse turns are structural motifs commonly found in proteins and bioactive peptides that, besides being fundamental in protein folding,[1] play a central role as molecular recognition elements for many biological processes. β-Turns are a subset of reverse turns and consist of a tetrapeptide sequence in a nonhelical region in which the chain direction is reversed. These turns are often stabilized by an intramolecular hydrogen bond between the carbonyl oxygen of the first residue (*i*) and the amide proton of the fourth one ($i + 3$), as shown in Figure 1.[1a,2] By virtue of presenting up to four side chains in a well-defined spatial arrangement, β-turns are often carriers of biological activity,[1a,3] thus being very important as starting points in the design of the so-called "turn-mimetics" for the development of new drugs.[4] During the past decade many efforts have been concentrated to synthesize new reverse turn inducers and study the conformational preferences of turn-analogues within protein secondary structure models.[5] Surprisingly, to our knowledge the only examples of bicycles belonging to [*x*.*y*.1] family reported so far are based on norbornene skeleton, which acts as reverse turn inducer and stabilizes β-sheet secondary structures without the aid of any hydrogen bond by virtue of its "U-shape".[6]

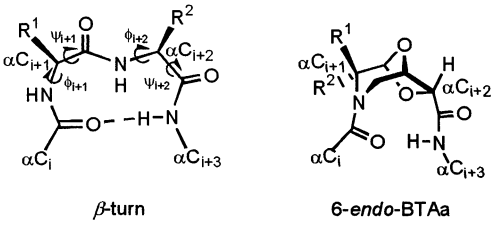

FIGURE 1. β-turn structure (left) and the isosteric replacement of $i + 1-i + 2$ dipeptidic sequence by 6-*endo*-BTAa (right).

In recent years we have developed a new class of azadioxa[3.2.1]bicyclic compounds named BTAa, which derive from the condensation of tartaric acid and amino acid derivatives.[7] We have previously described the potential

* To whom correspondence should be addressed. Tel.: 0039-055-4573481. Fax: 0039-055-4573569.
[†] Università di Firenze.
[‡] Università di Milano.
[§] Istituto di Chimica dei Composti Organo Metallici.

(1) Rose G. D.; Gierasch, L. M.; Smith J. A. *Adv. Prot. Chem*. **1985**, *37*, 1−109. (b) Stanfield, R. L.; Fieser, T. M.; Lerner, R. A.; Wilson, I. A. *Science*, **1990**, *248*, 712−719. (c) Chou, P. Y.; Fasman, G. D. *J. Mol. Biol*. **1977**, *115*, 135−175. (d) Wilmot, C. M.; Thorton, J. M. *J. Mol. Biol*. **1988**, *203*, 221−232. (e) Lewis, P. N.; Momany, F. A.; Scheraga, H. A. *Biochim. Biophys. Acta* **1973**, *303*, 211−229.
(2) Belvisi L.; Gennari C.; Mielgo A.; Potenza D.; Scolastico C. *Eur. J. Org. Chem*. **1999**, 389−400.
(3) Richardson, J. S. *Adv. Protein Chem*. **1981**, *34*, 167−339. (b) Müller, G. *Angew. Chem*. **1996**, *108*, 2941−2943; *Angew. Chem., Int. Ed. Engl*. **1996**, *35*, 2767−2769.
(4) Cho, N.; Harada, M.; Imaeda, T.; Imada, T.; Matsumoto, H.; Hayase, Y.; Sasaki, S.; Furuya, S.; Suzuki, N.; Okubo, S.; Ogi, K.; Endo, S.; Onda, H.; Fujino, M. *J. Med. Chem*. **1998**, *41*, 4190−4195. (b) Souers, A. J.; Virgilio, A. A.; Schürer, S. S.; Ellman, J. A.; Kogan, T. P.; West, H. E.; Ankener, W.; Vanderslice, P. *Bioorg. Med. Chem. Lett*. **1998**, *8*, 2297−2302. (c) Souers, A. J.; Virgilio, A. A.; Rosenquist, Å.; Fenuik, W.; Ellman, J. A. *J. Am. Chem. Soc*. **1999**, *121*, 1817−1825.

10.1021/jo0202132 CCC: $22.00
Published on Web 09/18/2002

SCHEME 1

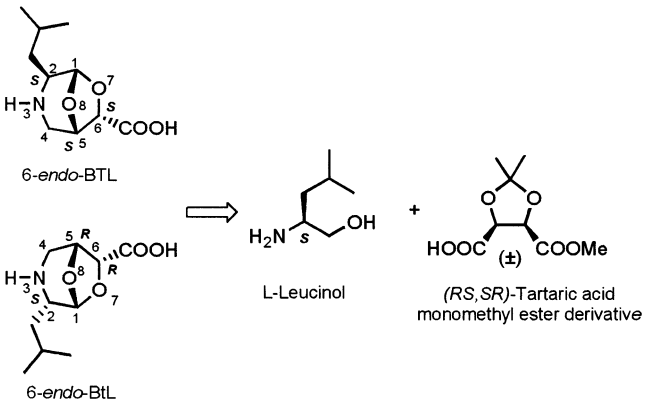

applications of these scaffolds as dipeptide isosteres when inserted in an open chain peptide.[7a] If *meso*-tartaric acid is used for the preparation of BTAa, the substituent at C-6 of BTAa scaffolds adopts an *endo* configuration and a subset of potential reverse turn inducers is obtained: in fact, the chair conformation of the six-membered ring locked in the bicyclic structure, in conjunction with the *endo* configuration at C-6 gives the right shape for imposing a reverse turn, thus replacing the $i + 1-i + 2$ dipeptidic sequence of a β-turn (Figure 1). Having demonstrated in a previous work that 6-*endo*-scaffolds are able to mimic the turn of a cyclic constrained peptide by replacing the X-Pro dipeptidic sequence,[8] we focused our attention on the possibility of BTAa to induce a reverse turn when inserted in a linear peptide chain without any further constraints.

The diastereomeric 6-*endo*-BTL and 6-*endo*-BtL scaffolds are obtained from L-leucinol and *(RS,SR)*-tartaric acid monomethyl ester derivative (Scheme 1) and show differences both in the absolute configuration at C-5 and C-6 carbon atoms of the *meso*-tartaric acid moiety, and in the relative disposition of leucine side chain at C-2 that is axial in the case of 6-*endo*-BTL and equatorial in the 6-*endo*-BtL scaffold. The two scaffolds were prepared as Fmoc-amino acids **1** and **2** (Scheme 2) and inserted in a linear hexapeptidic sequence by means of SPPS to give peptides Ac-Val-Ala-6-*endo*-BTL-Val-Gly-OMe **(3)** and Ac-Val-Ala-6-*endo*-BtL-Val-Gly-OMe **(4)**. Successively, the conformational analysis of peptides **3** and **4** was carried out by NMR and IR spectroscopy and by molecular modeling. Many examples are present in the literature about NMR experiments in which the hydrogen-bonding ability of amide NH protons is elucidated by dilution and temperature effects on chemical shift and by NOE effects which are diagnostic of structural preferences of reverse-turn peptides in solution.[9] Valine, alanine, and glycine were chosen as the amino acids to form the two β-strands on both sides of 6-*endo*-BT(t)L scaffolds since they satisfy the requirements of solubility in organic solvents (i.e. $CDCl_3$), lack of polar groups as possible competitors on intramolecular hydrogen bond formation, and absence of aromatic groups that might interfere during the study of amide protons by NMR.[10]

SCHEME 2

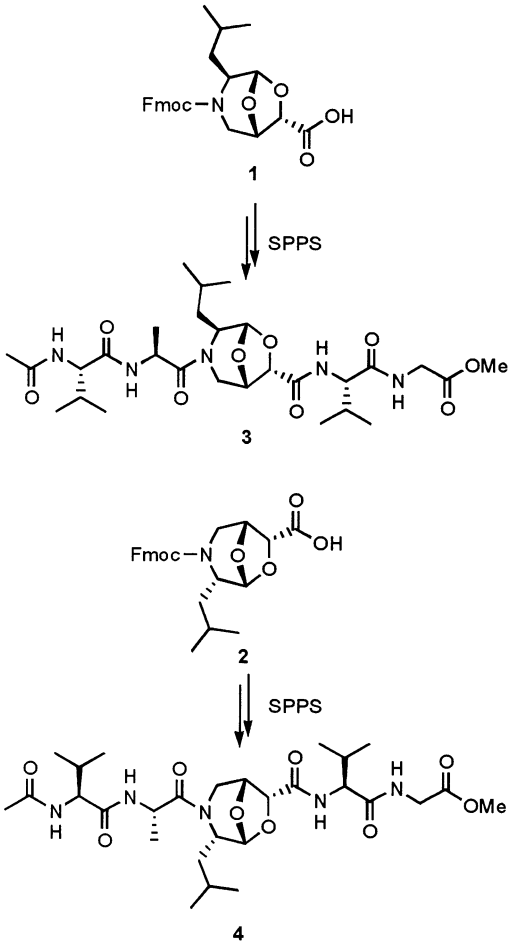

(5) Nagai, U.; Sato, K. *Tetrahedron Lett.* **1985**, *26*, 647−650. (b) Kemp, D. S.; Sites, W. E. *Tetrahedron Lett.* **1988**, *29*, 5057−5060. (c) Nagai, U.; Sato, K.; Nakamura, R.; Kato, R. *Tetrahedron* **1993**, *49*, 3577−3592. (d) Gardner, B.; Nakanishi, H.; Kahn, M. *Tetrahedron* **1993**, *49*, 3433−3448. (e) Giannis, A.; Kolter, T. *Angew. Chem., Int. Ed. Engl.* **1993**, *32*, 1244−1267. (f) Virgilio, A. A.; Ellman, J. A. *J. Am. Chem. Soc.* **1994**, *116*, 11580−11581. (g) Liskamp, R. M. J. *Recl. Trav. Chim. Pays-Bas* **1994**, *113*, 1−19. (h) Lombart, H.-G.; Lubell, W. D. *J. Org. Chem.* **1994**, *59*, 6147. (i) Gante, J. *Angew. Chem., Int. Ed. Engl.* **1994**, *33*, 1699−1720. (j) Schneider, J. P.; Kelly, J. W. *Chem. Rev.* **1995**, *95*, 2169−2187. (k) Gardner, R. R.; Liang, G.-B.; Gellman, S. H. *J. Am. Chem. Soc.* **1995**, *117*, 3280−3281. (l) Hanessian, S.; McNaughton-Smith, G.; Lombart, H.-G.; Lubell, W. D. *Tetrahedron* **1997**, *53*, 12789−12854. (m) Krauthäuser, S.; Christianson, L. A.; Powell, D. R.; Gellman, S. H. *J. Am. Chem. Soc.* **1997**, *119*, 11719−11720. (n) Feng, Y.; Pattarawarapan, M.; Wang, Z.; Burgess, K. *Org. Lett.* **1999**, *1*, 121−124. (o) Soth, M. J.; Nowick, J. S. *J. Org. Chem.* **1999**, *64*, 276−281. (p) Alonso, E.; López-Ortiz, F.; Del Pozo, C.; Peralta, E.; Macías, A.; González, J. *J. Org. Chem.* **2001**, *66*, 6333−6338.

(6) Ranganathan, D.; Haridas, V.; Kurur, S.; Thomas, A.; Madhusudanan, K. P.; Nagaraj, R.; Kunwar, A. C.; Sarma, A. V. S.; Karle, I. L. *J. Am. Chem. Soc.* **1998**, *120*, 8448−8460. (b) Hibbs, D. E.; Hursthouse, M. B.; Jones, I. G.; Jones, W.; Abdul Malik, K. M.; North, M. *J. Org. Chem.* **1998**, *63*, 1496−1504. (c) Jones, I. G.; Jones, W.; North, M. *J. Org. Chem.* **1998**, *63*, 1505−1513.

(7) Guarna, A.; Guidi, A.; Machetti, F.; Menchi G.; Occhiato E. G.; Scarpi D.; Sisi S.; Trabocchi A. *J. Org. Chem.* **1999**, *64*, 7347−7364. (b) Guarna, A.; Cini, N.; Machetti, F.; Menchi, G.; Occhiato, E. G. *Eur. J. Org. Chem.* **2002**, 873−880.

(8) Scarpi, D.; Occhiato E. G.; Trabocchi, A.; Leatherbarrow R. J.; Brauer A. B. E.; Nievo M.; Guarna A. *Bioorg. Med. Chem.* **2001**, *9*, 1625−1632.

(9) See, for example: (a) Stevens, E. S.; Sugawara, N.; Bonora, G. M.; Toniolo, C. *J. Am. Chem. Soc.* **1980**, *102*, 7048−7050. (b) Boussard, G.; Marraud, M. *J. Am. Chem. Soc.* **1985**, *107*, 1825−1828. (c) Gellman, S. H.; Dado, G. P.; Liang, G.-B.; Adams, B. R. *J. Am. Chem. Soc.* **1991**, *113*, 1164−1173. (d) Liang, G.-B.; Rito, C. J.; Gellman, S. H. *J. Am. Chem. Soc.* **1992**, *114*, 4440−4442. (e) Haque, T. S.; Little, J. C.; Gellman, S. H. *J. Am. Chem. Soc.* **1996**, *118*, 6975−6985. (f) Yang, J.; Gellman, S. H. *J. Am. Chem. Soc.* **1998**, *120*, 9090−9091.

(10) Huck B. R.; Fisk, J. D.; Gellman S. H. *Org. Lett.* **2000**, *2*, 2607−2610.

SCHEME 3[a]

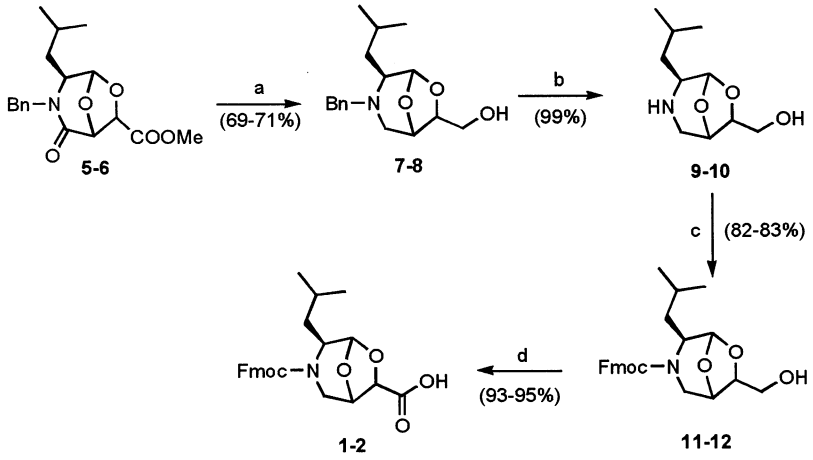

[a] Key: (a) $LiAlH_4$, THF, reflux, 2 h; (b) H_2, $Pd(OH)_2/C$, MeOH, 12 h; (c) Fmoc-*O*-Su, H_2O, acetone, Na_2CO_3, 0 °C, then 25 °C, 18 h; (d) Jones reagent, acetone, 0 °C, the 25 °C, 18 h.

Results and Discussion

Synthesis of *N*-Fmoc-amino Acids. Compounds **1** and **2** required for the synthesis of the target peptides **3** and **4**, respectively, were prepared following the general procedure for the synthesis of BTAa[7a] (Scheme 3). The starting amido esters **5** and **6**[11] were completely reduced with $LiAlH_4$ to give amino alcohols **7** and **8**, respectively, in good yields. Successively, debenzylation by $Pd(OH)_2/C$ catalyzed hydrogenolysis and subsequent protection of the amine function of the resulting compounds **9** and **10** with Fmoc-*O*-Su afforded the corresponding *N*-Fmoc-amino alcohols **11** and **12**. The final oxidation was carried out with Jones reagent. The crude *N*-Fmoc-amino acids **1** and **2** were carefully purified by FCC thus obtaining the title compounds in fair yields and without any trace of epimers at C-6, as evidenced by NMR.

Peptide Synthesis. Peptides **3** and **4** (Scheme 2) were prepared by means of a solid-phase peptide synthesis on a Wang resin using HBTU/HOBt chemistry except for the coupling of the amine and carboxyl functions of the 6-*endo*-BT(t)L scaffolds, which required different conditions due to their relative low reactivity, as already observed for similar BTAa.[8] Specifically, DIPC/HOBt activators were employed, and DIPEA was replaced by 2,4,6-collidine for alanine coupling to avoid C-α epimerization.[12] Peptide couplings on the amine and carboxyl functions of the scaffolds were repeated twice, and the reaction times were prolonged up to 3 days. All the peptide syntheses were monitored with ninhydrin following the Kaiser's method;[13] in the case of the secondary amine of the bicyclic scaffolds, bromophenol blue[14] and chloranil[15] tests were found to be not reliable. Despite the drastic conditions employed during the synthesis, the preparation of peptide **3** afforded, after TFA cleavage from the resin, a mixture of the desired compound as peptide acid and the Ac-6-*endo*-BTL-Val-Gly-OH byproduct due to incomplete coupling, as observed by ESI-MS and HPLC. The two compounds were separated by semipreparative HPLC. Final esterification with diazomethane and further HPLC purification afforded pure **3**. In the case of **4** the crude peptide was cleaved off the resin, and then it was directly esterified with diazomethane and purified by flash chromatography, which furnished a peptide with a better purity grade, although in lower yield.

Conformational Analysis of Peptide 3. Conformational studies on peptides **3** and **4** were performed by NMR, using a relatively nonpolar solvent (i.e. $CDCl_3$) in order not to interfere in the hydrogen bonding of amide protons. For ease of discussion only C-α and amide protons were numerated as well as the hydrogens of the scaffold. TOCSY and NOESY spectra were recorded to assign proton resonances and investigate both sequential and long-range NOE's that provide evidences of preferred conformations and give insight into stable *β*-hairpinlike conformations.[16] Temperature dependence experiments were carried out since the amide proton chemical shifts are sensitive to temperature and dilution variations, thus giving further insight into the conformational preferences of peptides. The combination of chemical shift and $\Delta\delta/\Delta T$ coefficient of amide protons provides information on the extent of hydrogen bonding.[2,9]

The ^1H NMR of peptide **3** showed two distinct sets of proton resonances in a 3:1 ratio clearly visible in the chemical shift range of the amide hydrogens. This is due to the presence of rotamers about the alanine-6-*endo*-BTL amide bond that do not interconvert at room temperature, as evinced in a previous work for similar compounds.[17] By comparison of chemical shift values of

(11) The preparation of scaffolds **5** and **6** for the synthesis of amino acids **1** and **2** was accomplished according to the general procedure previously reported (see ref 7a), having introduced some improvements concerning the oxidation of the alcohol obtained from the condensation of *N*-benzylleucinol with *meso*-tartaric acid monoester derivative. This was carried out by Dess–Martin periodinane, that was found to be more efficient than the Swern methodology used so far because of both easier synthetic procedure and absence of epimerization at C-α of the leucine mojety.

(12) Gennari, C.; Mielgo, A.; Potenza, D.; Scolastico, C.; Piarulli, U.; Manzoni, L. *Eur. J. Org. Chem.* **1999**, 379–388.

(13) Kaiser, E.; Colescott, R. L.; Bossinger, C. D.; Cook, P. I. *Anal. Biochem.* **1970**, *34*, 595–598.

(14) Krchnák, V.; Vágner, J.; Safár, P.; Lebl, M. *Collect. Czech. Chem. Commun.* **1988**, *53*, 2542–2548.

(15) Christensen, T. *Acta Chem. Scand.* **1979**, *B33*, 763–766.

(16) Sieber, V.; Moe, G. R. *Biochemistry* **1996**, *35*, 181–188.

(17) Machetti, F.; Ferrali, A.; Menchi, G.; Occhiato, E. G.; Guarna, A. *Org. Lett.* **2000**, *2*, 3987–3990.

TABLE 1. NOESY Cross-Peaks Observed for Peptides 3 and 4

Ac-Val[1]-Ala-6-*endo*-BT(t)L-Val[2]-Gly-OMe						
	3				**4**	
	major conformer		minor conformer			
residue	proton	NOE's	proton	NOE's	proton	NOE's
valine 1	N−H		N−H		N−H	
alanine	N−H	Ala α-H Val[1] α-H	N−H	Val[1] α-H, *β*-H Ala α-H, *β*-H; Val[2] N−H	N−H	Ala α-H; Val[1] α-H, *β*-H
6-*endo*-BT(t)L	H-1		H-1		H-1	
	H-2		H-2	Ala α-H	H-2	
	H-4	Ala α-H	H-4		H-4	Ala α-H, *β*-H
	H-5		H-5		H-5	
	H-6		H-6		H-6	
valine 2	N−H	H-6	N−H		N−H	Val[2] α-H; Leu *β*-H, *γ*-H
glycine	N−H		N−H		N−H	Val[2] α-H

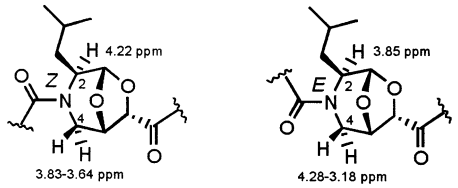

FIGURE 2. *E* and *Z* rotamers at alanine-6-*endo*-BTL amide bond, and C═O effect on 2-H and 4-H chemical shifts.

protons at C-2 and C-4 in the two rotamers it was possible to establish that the major conformer possesses a *Z* configuration at the alanine-6-*endo*-BTL bond. In fact, the amide C═O bond determines a strong downfield shift of the proton at C-2 in the *Z* rotamer and the protons at C-4 in the *E* rotamer (Figure 2). Despite the isocronousity of the 7-H proton of the two rotamers in the NOESY spectrum, the presence of NOE cross-peaks between 4-H and 7-H in the major conformer and between 2-H and 7-H in the minor one, and the absence of NOE's between 2-H and 7-H in the former rotamer and between 4-H and 7-H in the latter, confirmed that the major conformer possesses a *Z* configuration at alanine-6-*endo*-BTL amide bond (Figures 3a and 4a and Table 1). The absence of significant NOE's in the NOESY spectrum indicated that in the *Z* rotamer the structure is mainly in an open reverse turn conformation which is operated by the particular structural asset of 6-*endo*-BTL scaffold. NOE cross-peaks between 11-H and 6-H suggested that the C═O group of the scaffold has a certain rotational freedom and points inside the turn (Figure 3a). The temperature dependence ^{1}H NMR experiments showed the presence of equilibrating structures (Figure 3b and Table 2). Amide 11-H should not form any hydrogen-bond because of low values of both chemical shift and $\Delta\delta/\Delta T$. The chemical shift and $\Delta\delta/\Delta T$ values of glycine amide proton 13-H indicated an equilibrium between the hydrogen-bonded state and non-hydrogen-bonded states, suggesting either a *γ*-turn conformation as a consequence of weak interactions, or a hydrogen bond with an acetyl group that determines a strand orientation in accordance with NOE's. The data concerning the other amide protons 8-H and 10-H indicated the predominance of non-hydrogen-bonded states.

The minor conformer of peptide **3**, having a *E* configuration at the alanine-6-*endo*-BTL amide bond, showed a better organized structure. The NOESY spectrum showed sequential NOE cross-peaks between 8-H, 7-H, and 9-H indicating a *β*-strand organization of the *N*-terminal main chain (Table 1 and Figure 4a, left). Amide 11-H was found to be internal to the peptide turn in accordance with the cross-strand NOE cross-peak between 11-H and 8-H, that demonstrates the presence of a tight reverse turn. The temperature dependence experiments (see Table 2 and Figure 4b) suggested the presence of equilibrating structures, too. Amide 8-H is involved in an equilibrium between a non-hydrogen-bonded state and a strong intramolecular hydrogen-bonded 14-membered ring of *β*-hairpinlike structure, with rigidity like that observed in a classical *β*-hairpin hydrogen-bonded 10-membered ring. Glycine amide proton 13-H displayed weak hydrogen bonding in equilibrium with a non-hydrogen-bonded state, according to relatively large chemical shift and $\Delta\delta/\Delta T$ values, probably generating a *γ*-turn with the C═O group of the scaffold, in analogy with *Z* rotamer (Figure 4a, right).

IR spectroscopy was taken into account to distinguish between amide hydrogen-bonded and non-hydrogen-bonded states. The Ac-6-*endo*-BTL-NHMe monomer was chosen as reference compound, as it cannot experience intramolecular hydrogen bonding. The N−H stretching region for this compound displays a single N−H band, at 3430 cm^{-1}. At room temperature, in the infrared spectra of a 7 mM sample of compound **3** in $CHCl_3$ the non-hydrogen-bonded NH stretching vibrations appear as a narrow band at 3418 cm^{-1}, while the hydrogen-bonded NH stretching vibrations appear as a broad band at 3307 cm^{-1}.

Molecular modeling calculations using AMBER*[18] as a force field were carried out to gain further insight into the conformational preferences of peptides **3** and **4**. Two different Monte Carlo conformational searches were performed for the *E* and *Z* rotamers of compounds **3** and **4**. The distance *d* and the virtual torsion angle *β* were computed to investigate the turn propensity. The distance *d* between the C-α of the first and fourth residue of a *β*-turn is diagnostic of the presence of a reverse turn when its value is lower than 7 Å,[1a] and the virtual torsion angle *β* is indicative of a reverse turn when it assumes a value within the range of 0° ± 30°.[19] Considering the

(18) Mohamadi, F.; Richards, N. G.; Guida, W. C.; Liskamp, R.; Lipton, M.; Caufield, C.; Chang, G.; Hendrickson, T.; Still, W. C. *J. Comput. Chem.* **1990**, *11*, 440−467.

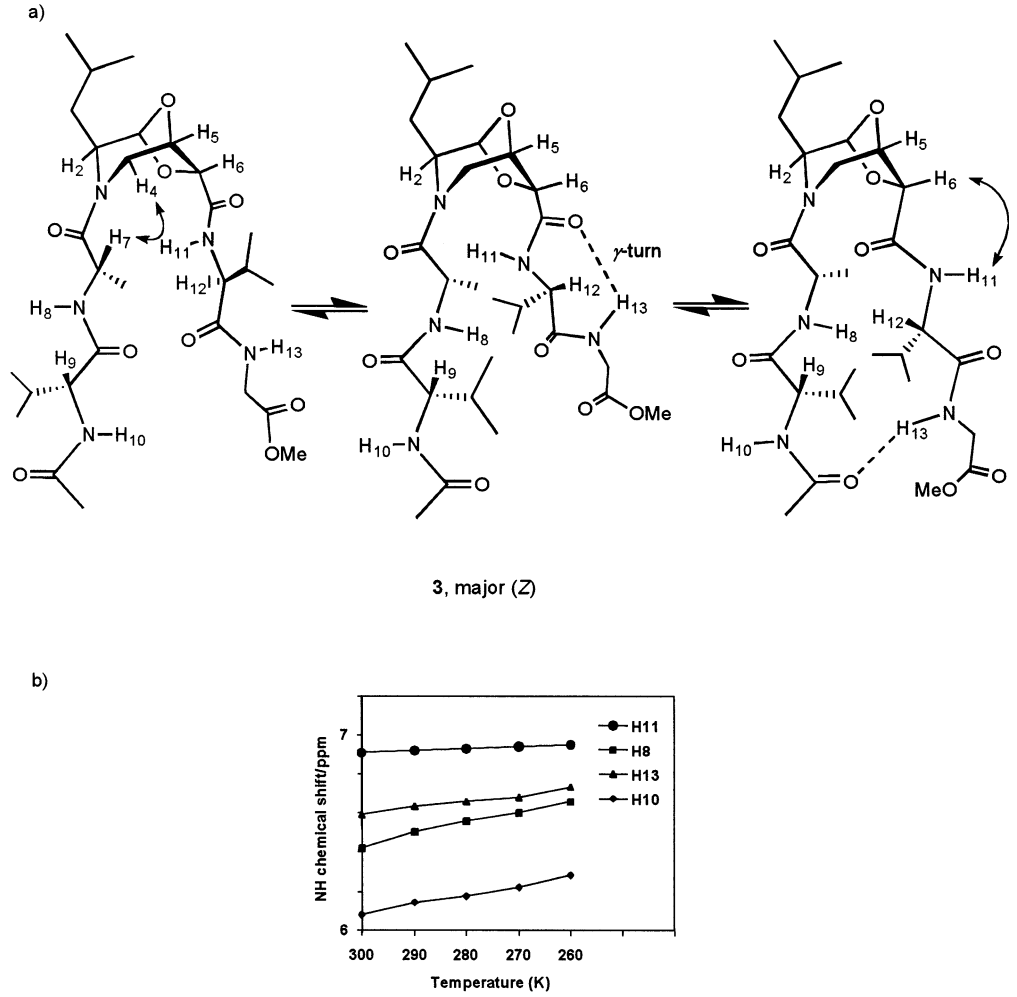

FIGURE 3. (a) Equilibrating structures of **3**, major conformer; the arrows indicate the NOE correlations. (b) Amide proton chemical shifts of peptide **3**, major conformer as a function of temperature.

TABLE 2. ^{1}H NMR Data for Amide Protons of Peptides 3 and 4 Recorded Using $CDCl_3$ Solutions[a,b]

Ac−Val-Ala-6-*endo*-BT(t)L-Val-Gly-OMe						
	3, major conformer		**3**, minor conformer		**4**	
	δ	$\Delta\delta/\Delta T$	δ	$\Delta\delta/\Delta T$	δ	$\Delta\delta/\Delta T$
8-H	6.42	−6.0	7.88	−5.25	6.75	−5.6
10-H	6.10	−5.0	6.42	−1.5	6.25	−14.86
11-H	6.91	−1.0	6.83	−5.0	7.21	−1.8
13-H	6.59	−3.5	7.16	−6.25	6.87	−23.2

[a] The chemical shifts δ are expressed in ppm, and $\Delta\delta/\Delta T$ coefficients in ppb/K. [b] The $\Delta\delta/\Delta T$ coefficients were determined between 260 and 300 K for peptide **3**, and between 250 and 300 K for peptide **4**.

6-*endo*-BT(t)L scaffolds as mimics of the $i + 1-i + 2$ central elements of a β-turn, the dihedral angle formed by the alanine carbonyl carbon, C-2 and C-6 of the scaffolds and nitrogen of valine next to the scaffold was taken into account. The conformational search on *Z* rotamer of peptide **3** (i.e. the major conformer) resulted in all the conformers having a marked tendency of adopting a reverse turn conformation, in which the scaffold occupies the central turn position (Figure 5). The global minimum conformer displayed an open turn structure with no intramolecular hydrogen bonds, and this structure was found in 54% of conformers (Figure 5a). In 12% of the conformers a γ-turn between 13-H and carbonyl group at C-6 of the scaffold was observed, in accordance with hydrogen-bonding of 13-H which is stabilized when the rotational freedom is reduced at low temperatures (Figure 5b). Moreover, in 34% of conformers with higher energy relative to the global minimum conformer, a structure having two hydrogen bonds formed by 8-H and 13-H was present (Figure 5c), that is congruent with NOE cross-peak between 6-H and 11-H (calculated distance of 2.20 Å), and with the presence of weak interactions stabilized at lower temperatures. As illustrated in Figure 5d,e, in which is represented the distribution of all the conformers found in the Monte Carlo conformational search versus β and *d* values,[20] all the structures found showed a turn conformation, as evidenced by the *d* value, but only 35% displayed β values in the range of 0° ± 30° and 92% in 0° ± 60° range, in agreement with the open turn structure. The molecular mechanic calculations on *E* rotamer confirmed the presence of a reverse turn and a better organized structure.

(19) Ball, J. B.; Hughes, R. A.; Alewood, P. F.; Andrews, P. R. *Tetrahedron* **1993**, *49*, 3467−3478.

(20) Müller, G.; Hessler, G.; Decornez, H. Y. *Angew. Chem., Int. Ed.* **2000**, *39*, 894−896.

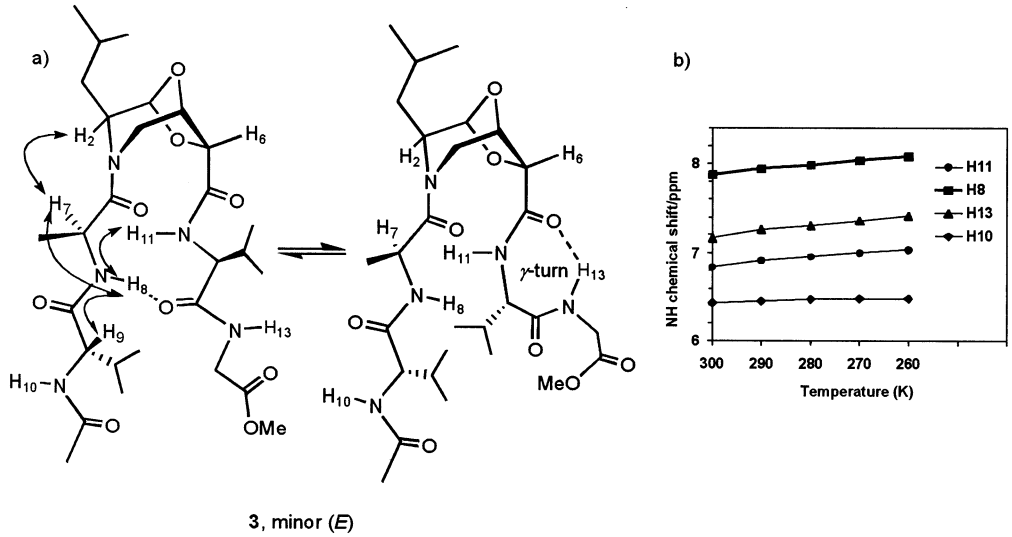

FIGURE 4. (a) Equilibrating structures of **3**, minor conformer; the arrows indicate the NOE correlations. (b) Amide proton chemical shifts of peptide **3**, minor conformer as a function of temperature.

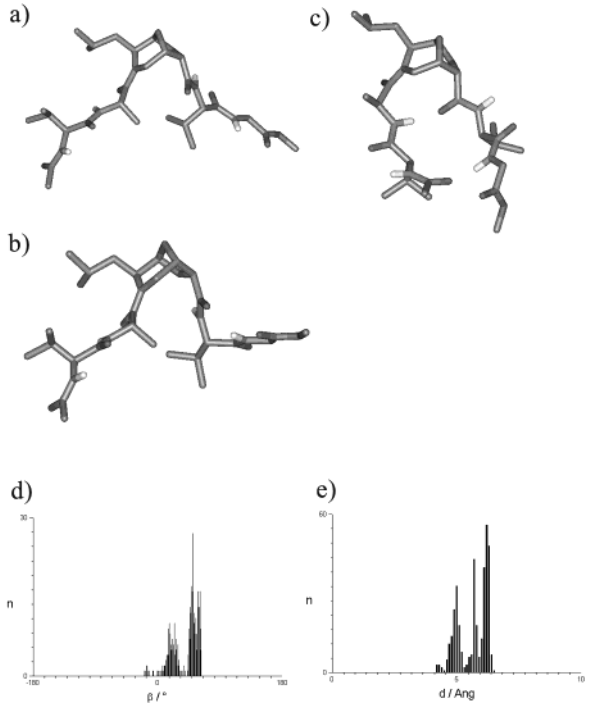

FIGURE 5. 3D structures of peptide **3**, major conformer. (a) Global minimum conformer. (b) γ-turn structure. (c) β-Hairpinlike structure. (d) Distribution profile of β values. (e) Distribution profile of d values.

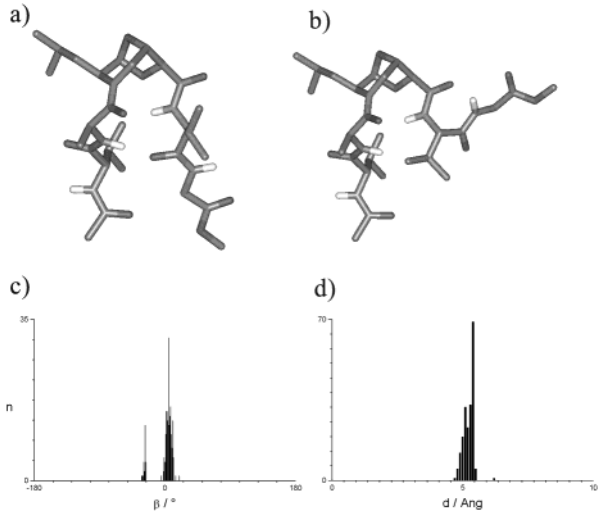

FIGURE 6. 3D structures of peptide **3**, minor conformer. (a) Global minimum conformer. (b) γ-Turn structure. (c) Distribution profile of β values. (d) Distribution profile of d values.

In 86% of conformers a 14-membered ring hydrogen bond between 8-H and the valine carbonyl group existed (Figure 6a). The calculated distance between 8-H and 11-H in the global minimum conformer was 2.35 Å, in agreement with the presence of a cross-strand NOE. Moreover, the presence of γ-turn conformers with intramolecular hydrogen-bonding was consistent with $\Delta\delta/\Delta T$ and chemical shift values of 13-H (Figure 6b). As illustrated in Figures 6c-*d*, in all the conformers the distance d is less than 7 Å, and 82% of the structures showed a turn conformation resulting in a virtual torsion angle below 30° in absolute value. Finally, it was found that the 10-membered ring hydrogen-bond formed by 11-H and the alanine C═O group cannot exist because of steric restrictions, and that in all the conformers the C-6 carbonyl group is fixed in an anti orientation.

Conformational Analysis of Peptide 4. A single set of amide hydrogens was found, which is consistent with the presence of a unique conformer. NOE cross-peaks between 7-H and 4-H *endo*, and between 4-H *exo* and methyl group of alanine, were indicative of *Z* configuration at alanine-6-*endo*-BtL amide bond (Table 1 and Figure 7a). This conformational restriction is probably due to a steric hindrance between the equatorial *sec*-butyl group at C-2 of 6-*endo*-BtL scaffold and the methyl group of alanine, thus resulting in a destabilization of the *E* rotamer. NOESY spectrum of peptide **4** showed several sequential NOE cross-peaks (Table 1 and Figure 7a) indicating that the two halves are organized into β-strands. The absence of any cross-strand NOE peaks suggested that the peptide folds in an open turn, probably because

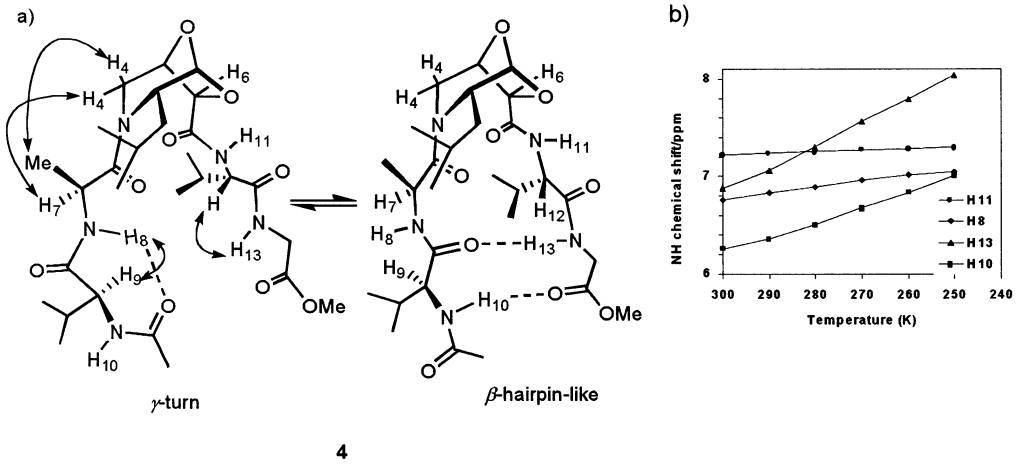

FIGURE 7. (a) Representation of peptide **4** equilibrating structures with selected NOE's. (b) Amide proton chemical shifts of peptide **4** as a function of temperature.

of the steric hindrance of bulky equatorial C-2 substituent that forces the six-membered ring of the scaffold into half-chair conformation, thus taking the two peptide halves away. The amide proton 11-H, despite its relatively high chemical shift and low $\Delta\delta/\Delta T$ value (Table 2 and Figure 7b), seemed not to form a hydrogen-bond but to remain in a fixed position as a consequence of antiperiplanar orientation of C═O group of the scaffold relative to C-6-O-7 bond. Alanine 8-H proton exhibited a weak hydrogen-bond probably involved in a γ-turn, and in equilibrium with a non hydrogen-bonded state, with the former being stabilized at lower temperatures (Figure 7a, left). The high $\Delta\delta/\Delta T$ coefficient calculated for 10-H and 13-H may indicate an equilibrium with a β-hairpinlike structure, in which two hydrogen bonds are formed at lower temperatures (Figure 7a, right). Thus, peptide **4** showed a unique conformer by virtue of steric effect produced by 6-*endo*-BtL, and it seemed to adopt an extended β-strands reverse turn conformation in analogy with the corresponding 6-*endo*-BTL modified peptide **3**.

Comparison of the N−H stretch region IR data for peptide mimics **4** and reference compound Ac-6-*endo*-BtL-NHMe indicated evidence of intramolecular hydrogen bonding in compound **4.** We assigned the hydrogen-bonded NH stretching vibrations at 3316 cm^{-1} while the free N−H appears at 3418 cm^{-1}.

The molecular mechanic resulted in a variety of conformers, all displaying a turn propensity. Only the *Z* conformer seemed to agree with NMR experiments, with the two peptide halves adopting an antiparallel conformation. All the conformers found showed an anti orientation of the scaffold's C═O group and the absence of hydrogen-bonding at 11-H amide proton, thus confirming that low $\Delta\delta/\Delta T$ and relatively high chemical shift values of 11-H amide proton (Table 2) are due to steric restrictions imposed by the scaffold that fixes 11-H in a well defined chemical environment. The global minimum conformer has the scaffold that occupies the central turn position, and 13.5% of the conformers found presented a γ-turn generated by a hydrogen bond between 8-H and the C═O of acetyl group (Figure 8a). Higher energy conformers showed a β-hairpinlike structure in which 10-H and 13-H are involved in two hydrogen bonds (Figure 8b), in accordance with the high $\Delta\delta/\Delta T$ values

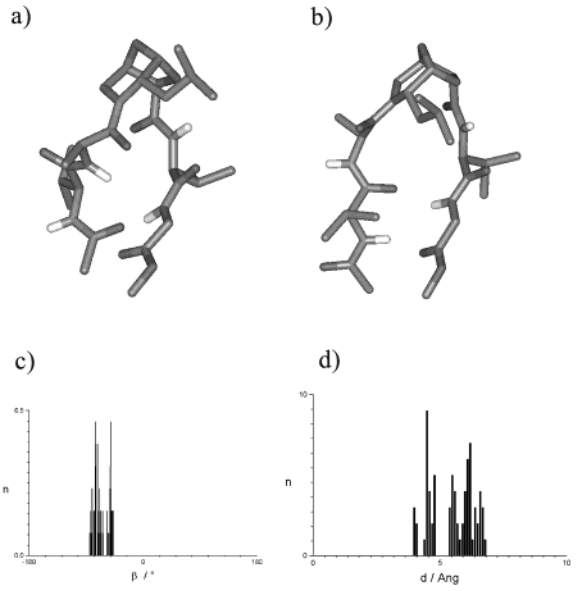

FIGURE 8. 3D structures of peptide **4**. (a) γ-Turn structure. (b) β-Hairpinlike structure. (c) Distribution profile of β values. (d) Distribution profile of *d* values.

of the two amide protons, thus indicating the stabilization of hydrogen bonding when rotational freedom is reduced at low temperatures. The plots of β and *d* values showed a broad range of populated values (Figure 8c,d) suggesting that peptide **4** does not exhibit a turn conformation as good as isomer **3**.

Conclusions

In this paper we have described the synthesis of two new 6-*endo*-BTL and 6-*endo*-BtL scaffolds having potential turn-inducing properties. We inserted the two molecules in a linear peptide in order to evaluate the ability of these scaffolds to constrain the peptide conformation in a reverse turn. We observed that the 6-*endo*-BTL molecule, having the leucine side chain in axial position, is a better reverse turn inducer since it can promote a tighter turn than the corresponding isomer which possesses the *sec*-butyl group of leucine in equatorial position. The two peptides **3** and **4** showed some hydrogen

bonding different from common β-turn structures, though this requirement was found to be not crucial for turn promotion. The absence of a 10-membered ring hydrogen-bond characteristic of β-turn structures indicates that the principal driving force for reverse turn formation is operated by the particular structural asset of the 6-*endo*-BT(t)L scaffold. Further stabilization is provided by intramolecular hydrogen bonding and hydrophobic interactions that contribute to the overall organization of a peptide into β-strand conformations.

NMR, IR, and molecular modeling analysis showed the presence of equilibrating structures due to amide hydrogens involved in equilibria between hydrogen-bonded and non-hydrogen-bonded states, with the former being stabilized by lowering the temperature. All the analyses led to the conclusion that 6-*endo*-BTAa scaffolds are able not only to retain a turn geometry, as previously demonstrated,[8] but also to provoke dramatic structural changes to a linear peptide chain due to their particular molecular construction. This effect can be modulated by either the position or the kind of functional group at C-2, as marked differences between the two 6-*endo*-BtL and 6-*endo*-BTL were observed. More precisely, the 6-*endo*-BTL scaffold seemed to act better as a reverse turn inducer, while 6-*endo*-BtL proved to impose severe structural restrictions resulting in a single preferred conformer irrespective of the stabilizing interactions produced by the two strands of the peptide.

Experimental Section

Melting points are uncorrected. Chromatographic separations were performed on silica gel using flash-column techniques; R_f values refer to TLC carried out on 25-mm silica gel 60 F_{254} plates with the same eluant indicated for column chromatography. ^{1}H and ^{13}C NMR spectra of all compounds but peptides **3** and **4** were recorded at 200 and 50.33 MHz, respectively. EI mass spectra were carried out at 70 eV ionizing voltage. THF was distilled from Na/benzophenone. CH_2Cl_2 was distilled from CaH_2. All reactions requiring anhydrous conditions were performed in oven-dried glassware. Acid silica gel (H_2SO_4/SiO_2) was prepared as reported.[21] All the solid-phase reactions were carried out on a shaker, using solvents of HPLC quality. All the compounds **5**−**12** were obtained with variable amounts (5−15%) of unseparable epimers at C-6. Only the final *N*-Fmoc-amino acids **1** and **2** were obtained as pure products and were fully characterized. Peptides **3** and **4** were purified by HPLC system equipped with semipreparative C18 10 μm, 250 × 10 mm, reverse-phase column using a H_2O−CH_3CN gradient eluant buffered with 0.1% TFA, and were characterized by ESI-MS and HPLC equipped with an analytical C18 10 μm, 250 × 4.6 mm, reverse-phase column.

NMR and IR Methods. NMR spectra of compounds **3** and **4** were acquired in $CDCl_3$ with an Avance 400 Bruker spectrometer. Solutions of 7 and 4.5 mM were employed for all conformational analyses of peptides **3** and **4**, respectively. ^{1}H NMR spectra for determining temperature coefficients were obtained at 260−300 K for **3** and at 250−300 K for **4**, with increments of 10 K. Complete proton resonance assignments of compounds **3** and **4** were made with TOCSY and NOESY experiments. IR spectra were recorded at room temperature with a FT-IR instrument.

Computational Methods. Molecular mechanic calculations were carried out on a SGI IRIX 6.5 workstation, using Macromodel (v6.5) molecular modeling software, with AMBER* as a force field and the implicit chloroform GB/SA solvation model.[22] The Monte Carlo conformational search was carried out without imposing any constraint and including amide bonds among all rotatable bonds. A ring closure bond was defined for the six- and seven-membered rings of the bicyclic 6-*endo*-BT(t)L scaffolds. Two thousand structures were generated and minimized. All the conformers having an energy of 6 kcal/mol above the global minimum conformer were discarded. The *E* and *Z* rotamers of each compound were separately analyzed.

(1*S*,2*S*,5*S*,6*R*)-3-Benzyl-2-*exo*-*sec*-butyl-6-*endo*-hydroxymethyl-7,8-dioxa-3-azabicyclo[3.2.1]octane (7). To a suspension of $LiAlH_4$ (232 mg, 6.12 mmol) in anhydrous THF (10 mL) was added dropwise at 0 °C under a nitrogen atmosphere a solution of **5** (680 mg, 2.04 mmol) in anhydrous THF (10 mL). The mixture was refluxed for 2 h, and then, after cooling at 0 °C, aqueous 0.4 N KOH (2 mL) and water (1 mL) were added and the suspension was refluxed for 30 min. The hot mixture was finally filtered through Celite and, after evaporation of the solvent, the crude product was purified by flash chromatography (CH_2Cl_2−MeOH, 30:1, R_f 0.4) giving pure **7** as a colorless oil (420 mg, 71%): ^{1}H NMR ($CDCl_3$) δ 7.32−7.20 (m, 5 H), 6.50 (br, 1 H), 5.37 (d, J = 1.5 Hz, 1 H), 4.26 (m, 1 H), 4.11 (d, J = 9.9 Hz, 1 H), 4.09 (s, 1 H), 3.84 (d, J = 10.6 Hz, 1 H), 3.58 (d, J = 2.2 Hz, 1 H), 2.92 (dd, J = 12.4, 2.2 Hz, 1 H), 2.78−2.72 (m, 2 H), 1.63−1.30 (m, 3 H), 0.87 (d, J = 6.3 Hz, 3 H), 0.59 (d, J = 6.2 Hz, 3 H); ^{13}C NMR ($CDCl_3$) δ 135.3 (s), 129.3 (d, 2 C), 128.3 (d, 2 C), 127.5 (d), 100.4 (d), 77.9 (d), 74.5 (d), 59.1 (t), 56.7 (t), 56.6 (t), 49.0 (t), 30.7 (t), 24.6 (d), 24.0 (q), 21.1 (q); MS *m*/*z* 291 (M^+, 20), 246 (100), 91 (100); IR ($CHCl_3$) 3142 (br) cm^{-1}. Anal. Calcd for $C_{17}H_{25}NO_3$: C, 70.07; H, 8.65; N, 4.81. Found: C, 69.47; H, 8.45; N, 4.68.

(1*R*,2*S*,5*R*,6*S*)-3-Benzyl-2-*endo*-*sec*-butyl-6-*endo*-hydroxymethyl-7,8-dioxa-3-azabicyclo[3.2.1]octane (8). Amino alcohol **8** was synthesized from **6** (579 mg, 1.74 mmol) as reported for **7**. Pure **8** (352 mg, 69%) was obtained after purification by flash chromatography as a yellow oil (CH_2Cl_2−MeOH, 30:1, R_f 0.35): ^{1}H NMR ($CDCl_3$) δ 7.31−7.19 (m, 5 H), 5.90 (br, 1 H), 5.34 (s, 1 H), 4.23 (m, 1 H), 4.05 (d, J = 14.6 Hz, 1 H), 4.02 (s, 1 H), 3.98 (d, J = 11.0 Hz, 1 H), 3.68 (d, J = 11.0 Hz, 1 H), 3.11 (d, J = 12.8 Hz, 1 H), 2.76 (d, J = 12.1 Hz, 1 H), 2.54 (dd, J = 12.1, 2.6 Hz, 1 H), 2.44 (dd, J = 9.2, 2.6 Hz, 1 H), 1.79−1.50 (m, 3 H), 0.95 (pseudo t, J = 6.2 Hz, 6 H); ^{13}C NMR ($CDCl_3$) δ 135.6 (s), 129.6 (d, 2 C), 128.3 (d, 2 C), 127.7 (d), 100.4 (d), 77.8 (d), 74.3 (d), 61.8 (d), 59.3 (t), 58.3 (t), 51.9 (t), 38.2 (t), 25.2 (d), 24.0 (q), 22.0 (q); MS *m*/*z* 291 (M^+, 6), 91 (100); IR ($CHCl_3$) 3168 (br) cm^{-1}. Anal. Calcd for $C_{17}H_{25}NO_3$: C, 70.07; H, 8.65; N, 4.81. Found: C, 69.95; H, 9.19; N, 4.75.

(1*S*,2*S*,5*S*,6*R*)-2-*exo*-*sec*-Butyl-6-*endo*-hydroxymethyl-7,8-dioxa-3-azabicyclo[3.2.1]octane (9). Compound **7** (403 mg, 1.38 mmol) was dissolved in MeOH (50 mL), 20% $Pd(OH)_2$/C (100 mg) was added, and the resulting suspension was left stirring at room temperature under a hydrogen atmosphere overnight. The catalyst was then removed by careful filtration over Celite and washed with MeOH. The solution was passed through a column filled with Amberlyst A-21 resin giving, after solvent evaporation, pure **9** (280 mg, 99%) as a viscous oil: ^{1}H NMR ($CDCl_3$) δ 6.05 (br, 2 H), 5.30 (s, 1 H), 4.31 (m, 1 H), 4.22−4.06 (m, 1 H), 4.11 (d, J = 12.8 Hz, 1 H), 3.92 (d, J = 12.8 Hz, 1 H), 3.42−3.10 (m, 3 H), 2.12−1.39 (m, 3 H), 0.91 (pseudo t, J = 6.4 Hz, 6 H); ^{13}C NMR ($CDCl_3$) δ 100.9 (d), 77.6 (d), 73.8 (d), 58.0 (t), 54.5 (d), 41.5 (t), 36.9 (t), 24.7 (d), 22.5 (q), 22.4 (q); MS *m*/*z* 201 (M^+, 3), 156 (100); IR ($CHCl_3$) 3198 (br) cm^{-1}. Anal. Calcd for $C_{10}H_{19}NO_3$: C, 59.68; H, 9.51; N, 6.96. Found: C, 59.45; H, 9.48; N, 6.91.

(1*R*,2*S*,5*R*,6*S*)-2-*endo*-*sec*-Butyl-6-*endo*-hydroxymethyl-7,8-dioxa-3-azabicyclo[3.2.1]octane (10). Prepared from **8** (352 mg, 1.21 mmol) as reported for **9**, affording pure **10** (240

(21) Guidi, A.; Guarna, A.; Macherelli, M.; Menchi, G. *Arch. Pharm. Med. Chem.* **1997**, *330*, 201−202.

(22) Still, W. C.; Tempczyk, A.; Hawley, R. C.; Hendrickson, T. *J. Am. Chem. Soc.* **1990**, *112*, 6127−6129.

TABLE 3. ^{1}H NMR Chemical Shifts of Peptides 3 and 4 Recorded in $CDCl_3$ Solutions

Ac−Val^1-Ala-6-*endo*-BT(t)L-Val^2-Gly-OMe															
	3, major					**3**, minor					**4**				
sequence	NH	C-α	C-*β*	C-*γ*	C-*δ*	NH	C-α	C-*β*	C-*γ*	C-*δ*	NH	C-α	C-*β*	C-*γ*	C-*δ*
Val 1	6.10	4.24	2.03	0.92	−	6.42	4.49	2.26	0.95	−	7.21	4.40	2.16	1.01	−
Ala	6.42	4.62	1.27	−	−	7.88	4.62	1.30	−	−	6.75	4.83	1.35	−	−
Val 2	6.91	3.92	2.10	1.00	−	6.84	4.01	2.26	1.02	−	6.25	4.32	2.05	0.93	−
Gly	6.59	4.05	−	−	−	7.16	4.14	−	−	−	6.87	4.17−4.00	−	−	−
Leu (BTtL)	−	−	1.55−1.26	1.27	0.94	−	−	1.33−1.85	1.68	1.01	−	−	1.75	1.57	1.01
H_1			4.73					4.70					4.88		
H_2			4.22					3.85					4.37		
H_4			3.64−3.83					4.28−3.18					4.02−3.25		
H_5			5.50					5.47					5.61		
H_7			4.52					4.47					4.46		
Ac			2.04					1.95 22.1					2.00		
OMe			3.77					3.77					3.76		

mg, 99%) as an oil: ^{1}H NMR ($CDCl_3$) δ 6.32 (br, 2 H), 5.25 (s, 1 H), 4.34 (m, 1 H), 4.17−4.04 (m, 2 H), 3.91 (d, J = 12.4 Hz, 1 H), 3.30 (AB system, J = 12.5 Hz, 2 H), 3.10 (t, J = 7.0 Hz, 1 H), 1.66 (m, 1 H), 1.38 (t, J = 7.3 Hz, 2 H), 0.88 (d, J = 2.9 Hz, 3 H), 0.85 (d, J = 2.6 Hz, 3 H); ^{13}C NMR ($CDCl_3$) δ 100.3 (d), 78.3 (d), 72.9 (d), 58.1 (d), 55.7 (d), 45.2 (t), 39.1 (t), 23.7 (d), 22.6 (q), 22.5 (q); MS *m*/*z* 201 (M^+, 9), 156 (100); IR ($CHCl_3$) 3207 (br) cm^{-1}. Anal. Calcd for $C_{10}H_{19}NO_3$: C, 59.68; H, 9.51; N, 6.96. Found: C, 59.63; H, 9.49; N, 6.93.

(1*S*,2*S*,5*S*,6*R*)-3-(9-Fluorenylmethoxycarbonyl)-2-*exo*-*sec*-butyl-6-*endo*-hydroxymethyl-7,8-dioxa-3-azabicyclo-[3.2.1]octane (11). Compound **9** (260 mg, 1.30 mmol) was suspended in a mixture of water (10 mL) and acetone (5 mL) containing Na_2CO_3 (138 mg, 1.30 mmol), and, after cooling to 0 °C, a solution of Fmoc-*O*-Su (482 mg, 1.43 mmol) in acetone (10 mL) was added. The mixture was stirred at room-temperature overnight, water (10 mL) was added, the aqueous phase was saturated with NaCl, and the organic products were extracted with CH_2Cl_2. After solvent evaporation, a solid product was obtained which was purified by flash chromatography (CH_2Cl_2−MeOH, 30:1, R_f 0.37), affording pure **11** (451 mg, 82%): ^{1}H NMR ($CDCl_3$) (mixture of rotamers) δ 7.67 (d, J = 7.0 Hz, 2 H), 7.51 (d, J = 7.0 Hz, 2 H), 7.35−7.20 (m, 4 H), 5.18 (s, 1 H), 4.66−3.07 (m, 10 H), 2.64 (br, 1 H), 1.60−1.10 (m, 3 H), 0.89−0.67 (m, 6 H); ^{13}C NMR ($CDCl_3$) δ 155.4 (s), 154.7 (s), 143.5 (s), 143.4 (s), 143.3 (s), 141.0 (s), 127.4 (d), 126.8 (d), 124.4 (d), 119.7 (d), 100.6 (d), 99.8 (d), 77.1 (d), 72.8 (d), 72.0 (d), 66.6 (t), 66.4 (t), 60.4 (t), 54.9 (d), 54.6 (d), 47.2 (d), 40.5 (t), 40.2 (t), 37.6 (t), 24.4 (d), 24.3 (d), 23.0 (q), 22.1 (q), 21.7 (q); ESI-MS *m*/*z* amu 424 (M^+ + 1, 100); IR ($CHCl_3$) 3163 (br), 1740 cm^{-1}. Anal. Calcd for $C_{25}H_{29}NO_5$: C, 70.90; H, 6.90; N, 3.31. Found: C, 70.96; H, 6.93; N, 3.28.

(1*R*,2*S*,5*R*,6*S*)-3-(9-Fluorenylmethoxycarbonyl)-2-*endo*-*sec*-butyl-6-*endo*-hydroxymethyl-7,8-dioxa-3-azabicyclo-[3.2.1]octane (12). Prepared from **10** (240 mg, 1.20 mmol) as reported for **11**, affording after purification by flash chromatography (CH_2Cl_2−MeOH, 30:1, R_f 0.4), pure **12** (421 mg, 83%) as a yellow oil: ^{1}H NMR ($CDCl_3$) δ 7.74 (d, J = 6.6 Hz, 2 H), 7.56 (d, J = 7.0 Hz, 2 H), 7.42−7.25 (m, 4 H), 5.38 (d, J = 3.3 Hz, 1 H), 4.61−4.41 (m, 2 H), 4.19 (t, J = 6.1 Hz, 1 H), 4.07−3.96 (m, 2 H), 3.87−3.79 (m, 1 H), 3.66−3.41 (m, 4 H), 2.71 (br, 1 H), 1.77−1.36 (m, 3 H), 0.84 (d, J = 6.2 Hz, 6 H); ^{13}C NMR ($CDCl_3$) δ 156.9 (s), 143.6 (s), 141.1 (s), 127.5 (d, 2 C), 126.8 (d, 2 C), 124.5 (d, 2 C), 119.8 (d, 2 C), 99.3 (d), 76.5 (d), 71.2 (d), 66.8 (t), 60.9 (t), 56.0 (d), 47.1 (d), 43.6 (t), 38.9 (t), 24.4 (d), 23.8 (q), 21.2 (q); ESI-MS *m*/*z* amu 424 (M^+ + 1, 100); IR ($CHCl_3$) 3375 (br), 1740 cm^{-1}. Anal. Calcd for $C_{25}H_{29}NO_5$: C, 70.90; H, 6.90; N, 3.31. Found: C, 70.92; H, 6.95; N, 3.24.

(1*S*,2*S*,5*S*,6*S*)-3-(9-Fluorenylmethoxycarbonyl)-2-*exo*-*sec*-butyl-7,8-dioxa-3-azabicyclo[3.2.1]octane-6-*endo*-carboxylic Acid (1). To a solution of **11** (440 mg, 1.04 mmol) in acetone (40 mL) was added Jones reagent[23] (7.7 mL, 6.24 mmol) dropwise at 0 °C, and the mixture was stirred at 0 °C for 40 min and at room temperature overnight. 2-Propanol was added until the color of the mixture turned green, and then it was filtered and evaporated to give a crude product which was directly purified by flash chromatography (CH_2Cl_2−MeOH−TFA, 30:1:0.03, R_f 0.13), affording pure **1** (422 mg, 93%) as a viscous oil: $[\alpha]^{23}_D$ −2.65 (*c* 0.49, $CHCl_3$); ^{1}H NMR ($CDCl_3$) (2:1 mixture of rotamers) δ 7.96−7.66 (m, 2 H), 7.62−7.48 (m, 2 H), 7.38−7.19 (m, 4 H), 5.41 (s, 0.3 H), 5.34 (s, 0.6 H), 4.66−3.69 (m, 7 H), 3.40−3.18 (m, 1 H), 1.69−1.19 (m, 3 H), 0.94−0.74 (m, 6 H); ^{13}C NMR ($CDCl_3$) δ 170.5 (s), 155.8 (s), 144.2 (s), 143.4 (s), 141.2 (s), 127.5 (d), 127.4 (d), 127.0 (d), 126.9 (d), 125.1 (d), 124.8 (d), 119.7 (d), 102.3 (d), 101.4 (d), 75.6 (d), 74.6 (d), 74.0 (d), 67.5 (d), 55.1 (d), 47.2, 41.7 (t), 41.3 (t), 37.8 (t), 24.6 (d), 23.0 (q), 22.1 (q); ESI-MS *m*/*z* amu 460 (M^+ + Na, 100), 438 (M^+ + 1, 70); IR ($CHCl_3$) 3435 (br), 1754, 1692, 1671 cm^{-1}. Anal. Calcd for $C_{25}H_{27}NO_6$: C, 68.63; H, 6.22; N, 3.20. Found: C, 68.59; H, 6.19; N, 3.25.

(1*R*,2*R*,5*R*,6*R*)-3-(9-Fluorenylmethoxycarbonyl)-2-*endo*-*sec*-butyl-7,8-dioxa-3-azabicyclo[3.2.1]octane-6-*endo*-carboxylic Acid (2). Prepared from **12** (415 mg, 0.98 mmol) as reported for **1**, giving after purification by flash chromatography (CH_2Cl_2−MeOH−AcOH, 40:1:0.03, R_f 0.2) pure **2** as a white solid (406 mg, 95%): mp 61−65 °C; $[\alpha]^{23}_D$ +65.7 (*c* 0.49, $CHCl_3$); ^{1}H NMR ($CDCl_3$) δ 7.70 (d, J = 7.0 Hz, 2 H), 7.50 (d, J = 7.0 Hz, 2 H), 7.45−7.22 (m, 4 H), 5.46 (d, J = 3.7 Hz, 1 H), 4.74 (br s, 1 H), 4.48−4.33 (m, 2 H), 4.16 (m, 1 H), 3.69 (m, 2 H), 3.33 (d, J = 13.5 Hz, 1 H), 1.76−1.67 (m, 3 H), 0.81 (m, 6 H); ^{13}C NMR ($CDCl_3$) δ 170.5 (s), 156.9 (s), 143.7 (s), 141.2 (s), 127.6 (d, 2 C), 127.0 (d, 2 C), 124.8 (d, 2 C), 119.9 (d, 2 C), 101.1 (d), 76.7 (d), 71.4 (d), 67.3 (t), 56.3 (d), 47.2 (d), 43.6 (t), 38.0 (t), 24.6 (d), 23.8 (q), 21.5 (q); ESI-MS *m*/*z* amu 460 (M^++Na, 100), 438 (M^++1, 61); IR ($CHCl_3$) 3340 (br), 1755, 1703, 1690 cm^{-1}. Anal. Calcd for $C_{25}H_{27}NO_6$: C, 68.63; H, 6.22; N, 3.20. Found: C, 68.59; H, 6.18; N, 3.27.

Ac-Val-Ala-6-*endo*-BTL-Val-Gly-OMe (3). Fmoc-Gly-Wang resin (86 mg, 64.5 μmol) was used as starting reagent. Fmoc deprotections were performed twice with 30% piperidine in DMF for 5 min, followed by resin washings with DMF. In case of primary amino groups coupling reactions were monitored with ninhydrin test.[13] Coupling of valine was performed using a 5-fold amino acid excess (110 mg, 0.32 mmol), a mixture of 0.5 M HBTU and 0.5 M HOBt as coupling reagents (0.65 mL, 0.32 mmol), and 1 M DIEA (0.65 mL, 0.65 mmol) as base, allowing the mixture to shake for 30 min. After Fmoc deprotection, peptide bound to resin was treated with an activating mixture of 0.14 M HOBt and 0.14 M DIPC in DMF (1.4 mL, 0.20 mmol), compound **1** (42 mg, 96 μmol), and 1 M DIEA (0.2 mL, 0.20 mmol), the mixture was allowed to shake for 3 days, and then the resin was washed with DMF and the coupling was repeated. After Fmoc deprotection, alanine was mounted

(23) Prepared by slow addition of concentrated H_2SO_4 (1.2 mL) to a cold solution of CrO_3 (624 mg) in H_2O (7.7 mL).

on peptide resin using 5-fold amino acid excess (100 mg, 0.32 mmol), 0.14 M HOBt, and 0.14 M DIPC in DMF (1.4 mL, 0.20 mmol) as activating mixture and 2,4,6-collidine as base (43 μL, 0.32 mmol), and the mixture was allowed to shake for 3 days. The free amino groups where then capped by treating the peptide bound to resin with Ac_2O (53 μL, 0.65 mmol) and 1 M DMAP in DMF (65 μL, 6.5 μmol) at room-temperature overnight. After resin washings with DMF and Fmoc deprotection, valine coupling was performed using a 5-fold amino acid excess (110 mg, 0.32 mmol), a mixture of 0.5 M HBTU and 0.5 M HOBt (0.65 mL, 0.32 mmol), and 1 M DIEA (0.65 mL, 0.65 mmol), leaving the mixture shaking for 30 min. After Fmoc deprotection and resin washings with DMF, resin was suspended in DMF (1 mL) and it was treated with Ac_2O (53 μL, 0.65 mmol) and 1 M DMAP in DMF (65 μL, 6.5 μmol) at room-temperature overnight. After resin washings with DMF, MeOH, and CH_2Cl_2, peptide acid was cleaved off the resin with 95% TFA (1.5 mL, 1 × 5 min, 1 × 2 h, 1 × 15 min), and then the mixtures were filtered, combined, and concentrated in vacuo to give crude peptide acid which was separated from the truncated Ac-6-*endo*-BTL-Val-Gly-OH peptide by semipreparative HPLC using 10−90% acetonitrile/55 min as gradient (t_R = 22.4 min). Peptide acid was dissolved in EtOAc and treated at 0 °C with a freshly prepared solution of diazomethane in Et_2O, the mixture was left stirring 1 h at room temperature, and excess of diazomethane was destroyed by AcOH addition. Crude peptide was purified by semipreparative HPLC using 10−90% acetonitrile/55 min as gradient (t_R = 26.6 min), giving pure **3** (8 mg, 21%), which was characterized by ESI-MS, and analytical HPLC using 10−90% acetonitrile/20 min as gradient (t_R = 11.6 min). ESI-MS *m*/*z* 620.4 (M^+ + Na, 100), 598.6 (M^+ + 1, 84). ^{1}H NMR data are shown in Table 3.

Ac-Val-Ala-6-*endo*-BtL-Val-Gly-OMe (4). Peptide **4** was prepared as reported for **3**, starting from Fmoc-Gly-Wang resin (203 mg, 0.15 mmol) and compound **2** (100 mg, 0.17 mmol) and using a different purification protocol. After cleavage from the resin, crude peptide acid was directly esterified with diazomethane and successively purified by flash chromatography (CH_2Cl_2−MeOH, 30:1, R_f 0.11), yielding pure **4** (7.5 mg, 8%), which was characterized by MS and analytical HPLC using 10−90% acetonitrile/20 min as gradient (t_R = 12.7 min). MS *m*/*z* 597 (M^+ + 1, 0.3). ^{1}H NMR data are shown in Table 3.

Acknowledgment. The authors thank COFIN 2000-2002 for financial support.

JO0202132